International Journal of Advanced Engineering and Technology Research
ISSN: 3106-8677 (Print), ISSN: 3106-8685 (Online) | Vol. 3, No. 2, 2026

A High-Precision Gas Emission Prediction Model for Deep Mining Working Faces

Yuheng Che

[1] State Key Laboratory of Coal Mine Disaster Prevention and Control, Chongqing 400037, China;

[2] China Coal Technology and Engineering Group, Chongqing Research Institute, Chongqing 400037, China

Abstract: In the context of deep coal mining, the highly nonlinear and uncertain characteristics of gas emission intensity pose severe safety threats to underground production operations. This study proposes a novel gas emission prediction model integrating Kernel Principal Component Analysis (KPCA), an Improved Crow Search Algorithm (ICSA) embedded with adaptive neighborhood search mechanism, and Support Vector Regression (SVR). First, multi-source data preprocessing procedures including outlier elimination and missing value imputation are implemented to construct a standardized, high-quality dataset. On this basis, KPCA is adopted to extract core nonlinear features from the complex influencing factor system of gas emission, which effectively eliminates information redundancy and significantly improves subsequent computational efficiency. Furthermore, the ICSA with enhanced global exploration and local exploitation balance is introduced to perform adaptive optimization on the hyperparameters of SVR, which fundamentally avoids the local optimum trap in traditional parameter tuning processes and remarkably promotes the generalization performance of the final established KPCA−ICSA−SVR prediction model. Comparative experimental results show that the proposed model outperforms all benchmark models in prediction accuracy and robustness, with the Root Mean Square Error (RMSE) measured at 0.17898 for the training set and 0.3071 for the testing set, fully verifying its outstanding applicability and reliability in dynamic gas emission prediction scenarios of deep working faces.

Keywords: Gas emission prediction, data preprocessing, prediction metrics, crow search optimization algorithm.

1. Introduction

Coal remains the dominant foundational energy source in China's energy consumption structure, underpinning critical sectors including power generation, heavy industry and freight transportation, due to its abundant domestic reserves, stable supply chain and relatively low cost advantage [1–3]. Nevertheless, with the continuous advancement of deep mining in recent years, the geological and hydrodynamic conditions of coal seams have become increasingly complex, leading to a sharp rise in the nonlinearity, dynamic fluctuation and uncertainty of gas emission behaviors, which has brought unprecedented severe safety challenges to underground coal production. Excessive gas emission will not only degrade the underground working environment and interfere with the normal operation of electromechanical equipment, but also cause rapid accumulation of gas in the restricted space of working faces and roadways, drastically increasing the explosion overrun risk, and posing a direct threat to the sustainable mining operation and occupational health of underground miners. Affected by multi-source coupled factors such as heterogeneous geological structures, variable coal seam gas content, different mining technologies and complex stress distribution, gas emission presents highly prominent time-varying characteristics, which makes the prediction performance of traditional empirical and linear statistical methods difficult to meet the actual safety production requirements of modern mines. In this context, realizing high-precision dynamic prediction of gas emission is an essential technical prerequisite for preventing and controlling gas disasters, and has important theoretical value and engineering significance for ensuring intrinsic safety of deep coal mines [4–8].

Scholars at home and abroad have carried out extensive in-depth research on gas emission prediction theories and technical methods, and have formed a series of representative research achievements. Guo et al. constructed a gas emission prediction model by integrating wavelet denoising algorithm and back propagation (BP) neural network, and verified the engineering applicability of the system through field measurement experiments [9]. Zhang et al. introduced Bootstrap resampling strategy, adopted out-of-bag (OOB) data scoring mechanism to complete model parameter tuning and feature importance evaluation, and finally determined the optimal hyperparameter set and the contribution proportionof each influencing factor for the prediction model [10]. Yan et al. extracted the core independent prediction indicators through factor analysis, and established a gas emission prediction model based on particle swarm optimization (PSO) optimized radial basis function (RBF) neural network [11]. However, existing mainstream prediction methods still have obvious inherent limitations: BP neural network is extremely sensitive to data noise and abnormal samples, and its iterative training process is prone to fall into local optimum; random forest (RF) model suffers from poor interpretability, which makes it difficult to quantitatively analyze the specific contribution of each influencing factor to gas emission; RBF neural network is faced with the serious "curse of dimensionality" problem when processing high-dimensional nonlinear data, which will lead to a significant decline in model prediction performance. In addition, most of the above models have deficiencies such as limited generalization ability, poor robustness under small sample conditions, and insufficient ability to mine complex nonlinear coupling relationships, which restrict their further improvement of prediction accuracy in complex deep mining scenarios [12–14].

Aiming at the multi-factor coupling, high-dimensional nonlinear and dynamic time-varying characteristics of gas emission in deep working faces, this study carries out

systematic method innovation and model construction. Firstly, complete data preprocessing procedures including abnormal sample elimination, missing value filling and standardized normalization are implemented, and a full-coverage evaluation index system covering geological, mining and gas parameters is established for gas emission prediction. To eliminate information redundancy among high-dimensional influencing factors, Kernel Principal Component Analysis (KPCA) is introduced to complete nonlinear feature extraction and dimensionality reduction, which retains the core information of original data while greatly reducing the dimension of input variables, and effectively improves the subsequent learning and training efficiency of the prediction model. On this basis, the standard Crow Search Algorithm (CSA) is improved by embedding adaptive neighborhood search and reinforcement learning mechanism, and the Improved CSA (ICSA) is adopted to perform global adaptive optimization on the hyperparameters of Support Vector Regression (SVR), which remarkably accelerates the algorithm convergence speed and avoids the risk of falling into local optimum. The finally constructed KPCA−ICSA−SVR prediction model can fully capture the complex nonlinear mapping relationship between gas emission and its multi-source influencing factors, and obtain more accurate and robust prediction results.

2. Formulation of Foundational Principles for Processes and Algorithms

2.1. Process for Establishing Predictive Models

The specific process for establishing a coal and gas outburst prediction model is as follows:

(1) Data Collection and Preprocessing: Gas emission data are collected and undergo comprehensive preprocessing. Outliers within the dataset are identified and removed using Boxplot analysis, thereby minimizing the impact of extreme values on model accuracy. Missing values are addressed through multiple imputation (MI), improving the completeness and quality of the data. Normalization is applied to remove scaling effects between features. Subsequently, Kernel Principal Component Analysis (KPCA) is employed for feature extraction and dimensionality reduction on the preprocessed data, retaining essential variable information while reducing dimensionality to optimize computational efficiency.

(2) Algorithm Optimization with Improved Crow Search (ICSA): An Improved Crow Search Algorithm (ICSA) is developed by integrating adaptive neighborhood search and reinforcement learning strategies. The adaptive neighborhood search adjusts search scopes dynamically, enhancing the algorithm's flexibility, while the reinforcement learning strategy accumulates experience to improve optimization efficiency and accuracy throughout the process. The ICSA's robust global and local search capabilities enable efficient exploration of the parameter space, fine−tuning the SVR model's hyperparameters, and yielding an optimal parameter set for gas emission prediction.

(3) Model Construction and Comparative Evaluation: After data preprocessing and hyperparameter optimization, comparative models are established to evaluate prediction effectiveness. Benchmark models such as BP, KPCA−ICSA−BP, and SVR are constructed. Evaluation metrics, including RMSE and MPE, are used to assess the performance of each model in gas emission prediction. Results indicate that the KPCA−ICSA−SVR model demonstrates a substantial advantage in prediction accuracy and generalization capability, capturing the nonlinear characteristics of gas emissions more effectively.

2.2. Basic Principles of the Algorithm

(1) Principal Component Analysis (PCA) is a classical dimensionality reduction technique that projects data into a lower−dimensional space via linear transformations, aiming to preserve as much of the original data's variance as possible. PCA is widely used in data preprocessing, feature extraction, and pattern recognition. However, the linear assumptions of PCA limit its effectiveness in handling complex, high−dimensional nonlinear data. In many real−world applications, data often exhibit significant nonlinearity, which constrains PCA's capacity to fully capture the inherent patterns and relationships within the data. To address this limitation, KPCA was developed. By incorporating kernel techniques, KPCA maps data into a high−dimensional feature space where nonlinear features can be more effectively captured using kernel functions such as the Gaussian or polynomial kernel. This approach enables principal component analysis in this new feature space, retaining the dimensionality reduction advantages of PCA while significantly enhancing its ability to model nonlinear structures. KPCA has demonstrated superior performance in fields like pattern recognition and data mining, effectively improving both the accuracy and robustness of data analysis.

The Crow Search Algorithm (CSA) is a population−based intelligent optimization algorithm inspired by the foraging behavior of crows. By simulating the memory and defense strategies of crows, the CSA searches for optimal solutions within the solution space. It is characterized by its simplicity and wide applicability, having demonstrated effective results across various optimization problems. However, the CSA tends to get trapped in local optima during the search process, and its balance between exploration and exploitation is limited, leading to slower convergence speeds and insufficient precision in complex, multi−modal, high−dimensional problems. To address these limitations, this study proposes an Improved Crow Search Algorithm (ICSA), which integrates adaptive neighborhood search and reinforcement learning strategies. First, adaptive neighborhood search dynamically adjusts the search radius of crows, ensuring flexibility in exploration during different search phases; this allows for extensive searching in the early stages while gradually focusing on fine−tuning in later stages. Furthermore, the incorporation of reinforcement learning allows the crows to adaptively select optimal search behaviors based on feedback from the environment, thereby enhancing the algorithm's decision−making capabilities. This improvement not only strengthens the CSA's global exploration capabilities and local search accuracy but also significantly increases convergence speed and solution precision, resulting in enhanced robustness and stability in tackling complex optimization problems.

(3) Support Vector Regression (SVR) is a regression model well suited for scenarios with small sample sizes and high−dimensional data. In gas emission prediction, where data collection is challenging and sample sizes are typically limited, traditional methods may struggle to achieve satisfactory accuracy under small sample conditions or in high−dimensional spaces. SVR constructs an optimal

regression hyperplane in the feature space, minimizing prediction error while controlling it within an ϵ−insensitive margin, providing strong generalization ability and robustness to small sample sizes. This approach effectively handles the nonlinearity and high−risk factors inherent in gas emission prediction, making it ideal for small−sample data analysis and significantly enhancing prediction accuracy and reliability.

3. Data Preprocessing

3.1. Data Acquisition

This study uses data from a coal mine's comprehensive mining face, where gas over−limit situations frequently occur. To prevent major disasters such as gas explosions, this research focuses on predicting gas outburst quantities in the mining face. A total of 30 representative data samples containing 12 influencing factors were obtained from the monitoring data of the mine to serve as the original dataset, as shown in Table 1.

In Table 1, the 12 influencing factors are as follows: coal seam burial depth x1 (m), coal seam gas content x2 (m3/t), coal seam thickness x3 (m), mining intensity x4 (t/d), working face recovery rate x5 (%), working face length x6 (m), coal seam dip angle x7 (°), adjacent layer gas content x8 (m3/t), adjacent layer thickness x9 (m), interlayer distance x10 (m), mining height x11 (m), and advance speed x12 (m/d); the gas outburst quantity is represented as y (m3/t). A total of 24 samples were randomly selected for the training set, while 6 samples were reserved for the testing set.

Table 1. Partial raw data

	x_1	x_2	x_3	x_4	x_5	x_6	x_7	x_8	x_9	x_{10}	x_{11}	x_{12}	y
1	408	2.04	2.4	1839	0.95	163	11	2.34	1.5	20	2.4	4.6	3.54
2	415	2.46	20.3	1639	0.96	158	11	2.42	1.23	21	2.3	4.54	4.07
3	430	2.4	2.1	1770	0.96		12	2.35	1.48	23	2.1	4	4.17
4	439	2.79	2.6	2091	0.95	149	12	2.45	1.81	19	2.6	4.76	4.56
5	460	2.71	2.6	2120	0.95	165	16	2.31	1.7	109	2.6	4.59	4.3
6	541	3.6	3.1		0.95	180	12	3.05	1.6	19	3.1	4	5.07
7	545	3.25	3.3	2006	0.95	168	13	2.46	1.6	20	3.3	3.93	4.64
8	608	4.04	3.55	2586	0.91	170	11	3.18	1.72	21	3.4	4.18	6.16
9	615	4.92	6.3	3395	0.802	172	12	3.3	1.6	14	6.3	3.39	7.58
…	…	…	…	…	…	…	…	…	…	…	…	…	
30	611	4.05	6.7	3354	0.812	175	9	3.15	1.8	16	6.7	2.64	7.8

3.2. Data Cleaning Based on Boxplot–MI

Table 1 presents the uncleaned data. MATLAB was used to clean the original dataset, beginning with the identification and handling of outliers using the Boxplot method. This involved calculating the lower and upper quartiles (Q1 and Q3) and the interquartile range (IQR) for each column of data, establishing upper and lower limits to identify which data points were outliers. These outliers were replaced with NaN to prevent them from affecting data analysis in subsequent processing. Next, multiple imputation (MI) was applied to fill in these missing values. In this study, six estimators were employed for imputing the missing values, including linear regression, logistic regression, decision trees (DTs), random forests (RFs), a support vector machine (SVM), and multilayer perceptrons. The root mean square error (RMSE) was used to evaluate the imputation results and determine the best estimator. They are particularly well suited for complex datasets and high−dimensional data. Therefore, this study selected an MLP as the estimator for MI data imputation. The complete data are presented in Table 2.

Table 2. Partial complete data

	x_1	x_2	x_3	x_4	x_5	x_6	x_7	x_8	x_9	x_{10}	x_{11}	x_{12}	y
1	408	2.04	2.4	1839	0.95	163	11	2.34	1.5	20	2.4	4.6	3.54
2	415	2.46	2.3	1639	0.96	158	11	2.42	1.23	21	2.3	4.54	4.07
3	430	2.4	2.1	1770	0.96	176	12	2.35	1.48	23	2.1	4	4.17
4	439	2.79	2.6	2091	0.95	149	12	2.45	1.81	19	2.6	4.76	4.56
5	460	2.71	2.6	2120	0.95	165	16	2.31	1.7	19	2.6	4.59	4.3
6	541	3.6	3.1	2250	0.95	180	12	3.05	1.6	19	3.1	4	5.07
7	545	3.25	3.3	2006	0.95	168	13	2.46	1.6	20	3.3	3.93	4.64
8	608	4.04	3.55	2586	0.91	170	11	3.18	1.72	21	3.4	4.18	6.16
9	615	4.92	6.3	3395	0.802	172	12	3.3	1.6	14	6.3	3.39	7.58
…	…	…	…	…	…	…	…	…	…	…	…	…	…
30	611	4.05	6.7	3354	0.812	175	9	3.15	1.8	16	6.7	2.64	7.8

3.3. Data Dimensionality Reduction Based on KPCA

Kernel Principal Component Analysis (KPCA) utilizes kernel functions to map data into a high−dimensional feature space, effectively extracting underlying nonlinear structures and complex features. This characteristic significantly enhances the accuracy and efficiency of data analysis when dealing with high−dimensional and complex datasets. Furthermore, KPCA not only reduces dimensionality to

improve the computational performance of models but also mitigates the impact of noise, thereby enhancing the expressive power of features.

Figure 1 shows the kernel matrix heatmap, which illustrates the similarity between data samples and reflects the structure of the kernel matrix calculated using a Gaussian kernel function. This heatmap provides a clearer analysis and identification of clustering trends and potential nonlinear relationships among the data samples. Each cell in the figure represents the similarity between two samples, with the color intensity indicating the level of similarity. Darker areas indicate high similarity, while lighter areas indicate low similarity. Clustering trends and potential nonlinear relationships between the samples can be visually identified. For instance, the similarity between the data in Group 1 and the data in Groups 2 and 3 is relatively high, as shown by the darker areas in the heatmap, indicating that these three groups exhibit similar patterns or behaviors in the feature space and are likely to belong to the same or nearby categories. In contrast, the similarity between the data in Group 1 and the data in Groups 10, 14, and 15 is low, as indicated by the lighter areas, suggesting significant differences between these samples and implying that they likely belong to different categories.

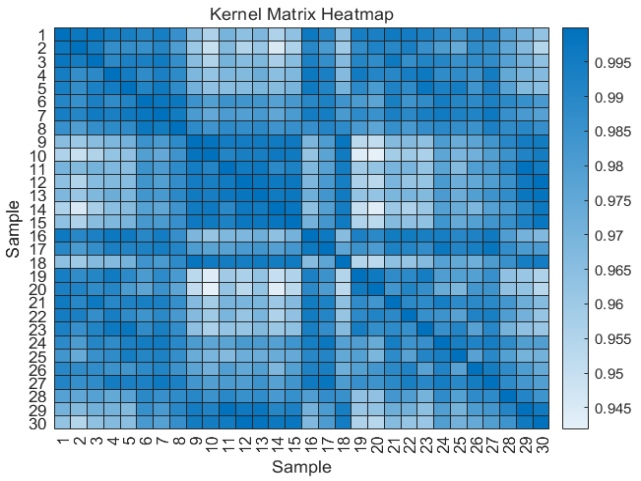

Figure 1. Kernel matrix heatmap

The variance explanation graph is shown in Figure 2, illustrating the proportion of total variance explained by each principal component. This graph serves as a tool for evaluating the importance and effectiveness of these components. The horizontal axis represents the component number, while the vertical axis shows the proportion of variance explained by each principal component. Typically, the first few principal components account for the majority of the variance, guiding the selection of an appropriate number of components to retain as much of the original data information as possible while reducing dimensionality and lowering computational complexity. Generally, a cumulative variance explanation ratio of 85% is considered a good balance between information retention and dimensionality reduction. In Figure 2, the cumulative variance explained by the first four principal components is calculated as 0.629978 + 0.116409 + 0.080876 + 0.062901 = 0.890164, which is greater than 0.85. Therefore, the first four principal components are selected for the reduced−dimensional data, with the reduced dataset presented in Table 3.

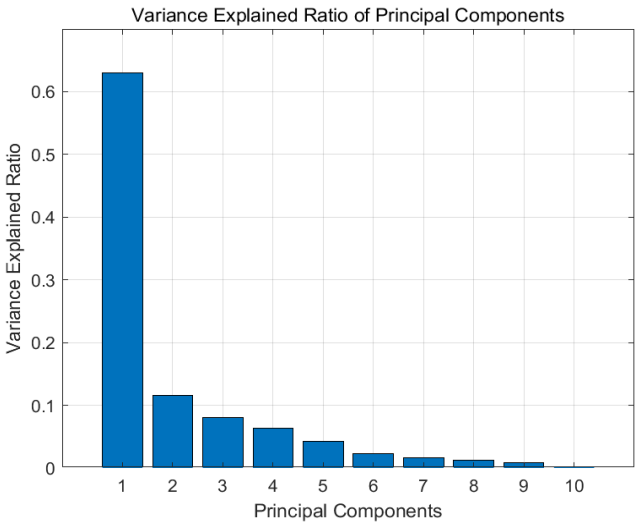

Figure 2. Variance explanation

Table 3. Partial data after dimensionality reduction

	P1	P2	P3	P4
1	−0.070030966	−0.007384908	0.001259093	−0.003374653
2	−0.075670036	−0.019152051	0.005231675	−0.007859444
3	−0.061941622	−0.001682007	0.003784321	−0.01279089
4	−0.057579009	0.005133138	−0.010676203	0.007044164
5	−0.0542516	0.018470685	−0.000564319	−0.002088861
6	−0.00737452	0.004864428	0.005790376	−0.010555114
7	−0.026565961	0.005300026	0.000784251	−0.004548474
8	0.009923864	0.002950055	−0.005103689	−0.00680728
9	0.080811222	−0.00030095	0.002270081	−0.001053749
…	…	…	…	…
30	0.085891336	−0.002544488	−0.005689592	0.001248051

4. Evaluation and Comparison of Models

4.1. Establishment of the KPCA−ICSA−SVR Prediction Model

Substituting the optimal hyperparameter values obtained from the ICSA optimization into the SVR model, a gas emission prediction model based on KPCA−ICSA−SVR is established. The training set prediction results are shown in Figure 3. As observed from the figure, the RMSE of the training set prediction reaches 0.17898, with an R2 of 0.9836, MAE of 0.1651, MSE of 0.032, and MAPE of 1.67%. All performance metrics are within reasonable ranges, indicating that the KPCA−ICSA−SVR model developed in this study for gas emission prediction is both reasonable and feasible.

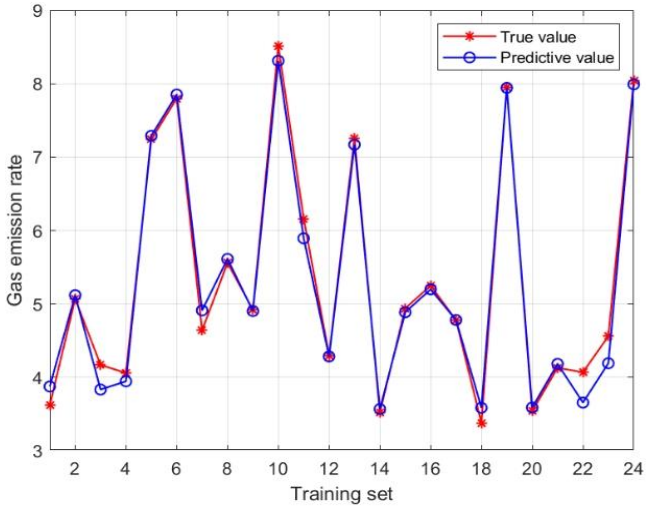

Figure 3. Training set prediction results

The test set prediction results are shown in Figure 4. From the figure, it can be observed that the RMSE of the test set prediction reaches 0.3132, indicating that the model's accuracy is within a reasonable range. This suggests that the KPCA−ICSA−SVR model does not exhibit overfitting or underfitting, demonstrating good generalization ability and enabling accurate predictions on new data.

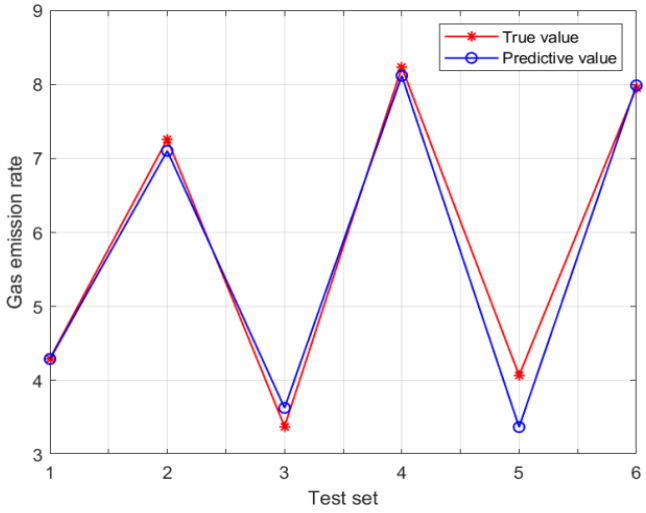

Figure 4. Test set prediction results

4.2. Test Set Performance Evaluation

To validate the superiority of the KPCA−ICSA−SVR model established in this study, three comparative models were constructed: BP neural network, KPCA−ICSA−BP, and SVR. Each model was applied to the test set for prediction, with the results presented in Table 4. Due to the small dataset size, the computation time for all models is within 15 s. As shown in the table, the KPCA−ICSA−SVR model outperforms others across all evaluation metrics. Notably, the addition of KPCA for dimensionality reduction and the ICSA to the BP model significantly enhanced its predictive accuracy, indicating that the KPCA−ICSA method can effectively optimize prediction models.

Table 4. Comparison of model prediction results.

Model	R^2	MAE	MAPE/%	MBE	RMSE	MPE/%
BP	0.8564	0.5017	6.56	0.4011	0.6041	4.51
KPCA−ICSA−BP	0.9252	0.3524	4.14	0.2519	0.4786	3.09
SVR	0.9436	0.2879	3.50	−0.1577	0.3568	−2.07
KPCA−ICSA−SVR	0.9752	0.2108	2.01	−0.1150	0.3071	−1.74

4.3. Model Safety Adjustment

Based on the model's prediction results, a safety margin is added to the predicted gas emission values (1):

$$\hat{y}_{\text{adjusted}} = \hat{y} + \Delta_{\text{safety}} \quad (1)$$

Where Δsafety is a safety adjustment value set based on historical data and expert experience to ensure early warnings under high−risk conditions. The calculation formula is as follows (2):

$$\Delta_{\text{safety}} = |\text{MBE}| + \alpha \quad (2)$$

Where α is a compensation coefficient determined by the historical extreme values of gas emissions and the risk tolerance level. To ensure sufficient conservativeness, this study sets α = 0.05, resulting in a Δsafety value of 0.165.

4.4. Model Generalization Verification

To evaluate the applicability of the proposed model, 30 sets of field data from the reference [11] were used for validation. The test mine, located at the 12,322 main working face, has an average coal seam thickness of 6.25 m, including one to two layers of carbonaceous mudstone and mudstone interlayers. In areas affected by geological structures, the coal seam thickness varies significantly, with faults extending into the working face. These factors—variations in coal seam thickness, faulting, and interlayer disruptions—can cause periodic fluctuations in gas emission. Moreover, fault damage and stress concentration zones may lead to sudden large gas emissions, increasing the risk of unexpected outbursts. Therefore, accurate gas emission prediction is essential to ensure safe and orderly mining operations.

The sample data include 11 indicators, such as daily production of the working face, interlayer lithology, and coal

seam thickness. The data samples were split into two groups; 80% were used for training and 20% for testing. The performance prediction results of different models are summarized in Table 5.

Table 5. Performance comparison.

Model		Maximum Error %	Minimum Error %	Average Error %
Reference [11]	RBF	16.29	0.77	7.28
	FA−PSO−RBF	11.64	0.25	5.65
	FA−AQPSO−RBF	9.27	0.22	2.59
This model	KPCA−ICSA−SVR	4.01	0.12	1.37

As shown in the table, the KPCA−ICSA−SVR gas emission prediction model established in this study outperforms the models referenced in the literature across all evaluation metrics. This demonstrates that the proposed model has good applicability to other coal seams.

5. Conclusions

(1) Data Cleaning and Feature Extraction: In this study, the Boxplot–MI method was employed for comprehensive data cleaning of gas emission data. After removing outliers with the Boxplot method, multiple imputation (MI) was used to handle missing data, ensuring data completeness and consistency. Next, Kernel Principal Component Analysis (KPCA) was used to extract key features and perform effective dimensionality reduction. The first four principal components, which explain a cumulative variance of 0.89016, were selected. This approach not only significantly simplified the data structure but also effectively preserved the essential information between variables.

(2) Model Optimization: An Improved Crow Search Algorithm (ICSA) was developed, integrating adaptive neighborhood search with reinforcement learning to optimize the SVR model's hyperparameters. By adaptively adjusting the neighborhood range and employing reinforcement learning strategies for dynamic exploration of the global optimum, the ICSA efficiently and stably identified the optimal parameter combination for SVR, enhancing model convergence speed and accuracy.

(3) Comparative Experiment: A series of comparative experiments, including BP, KPCA−ICSA−BP, and conventional SVR models, were conducted to assess each model's performance in gas emission prediction. Results demonstrated that the RMSE of the KPCA−ICSA−SVR model for the test set is 0.3132, which is lower than that of other models. Additionally, all other evaluation metrics show optimal performance, particularly in terms of prediction accuracy and generalization ability, surpassing the performance of other models.

Acknowledgment

This research was funded by the Key Scientific and Technological Program of the Ministry of Emergency Management (No. 2024EMST070703); General Program of Chongqing Natural Science Foundation (No. CSTB2025NSCQ-GPX0099); Self-funded Scientific Research and Development Project of China Coal Technology & Engineering Group Chongqing Research Institute Co., Ltd. (No. 2025YBXM40 and 2026YBXM06).

References

[1] Wu, Y., Wang, P., Wang, D., Bu, L., Tian, J., Sun, G., & Xu, S. (2024). Synergistic ductility deformation and helical design of carbon nanotube fiber composites. Carbon, 229, 119441.

[2] Wang, L., Sun, Y., Zheng, S., Shu, L., & Zhang, X. (2023). How efficient coal mine methane control can benefit carbon-neutral target: Evidence from China. Journal of Cleaner Production, 424, 138895.

[3] Harpalani, S., & Chen, G. (1995). Estimation of changes in fracture porosity of coal with gas emission. Fuel, 74, 1491–1498.

[4] Li, J., Xu, T., Lu, W., Zhao, X., He, Q., Li, J., & Zhuo, H. (2024). Water-gas masking effect of the primary active sites in coal and room temperature oxidation of coal after desorption. Journal of the China Coal Society, 49, 2298–2314.

[5] Wang, K., Li, K., Du, F., Zhang, X., Wang, Y., & Sun, J. (2024). Research on prediction model of coal spontaneous combustion temperature based on SSA-CNN. Energy, 290, 130158.

[6] Song, J., Deng, J., Zhao, J., Zhang, Y., Wang, C., & Shu, C. M. (2021). Critical particle size analysis of gas emission under high-temperature oxidation of weathered coal. Energy, 214, 118995.

[7] Wu, Y., Wang, P., Wang, D., Bu, L., Tian, J., & Xu, S. (2024). Unveiling the microstructural evolution and interaction mechanisms for twisted structures. International Journal of Mechanical Sciences, 279, 109514.

[8] Xie, J. (2024). Research on pre-pumping gas control technology for large-diameter borehole. Journal of Mining Science and Technology, 9, 529–537+652.

[9] Guo, X., Ren, Z., Wang, Q., & Cui, C. (2019). Prediction of gas emission by BP neural network based on wavelet analysis. IOP Conference Series: Earth and Environmental Science, 252, 052046.

[10] Zhang, Z., & Ma, W. (2023). Prediction of gas emission in mining face based on random forest regression algorithm. Journal of Mine Automation, 49, 33–39.

[11] Yan, H. (2020). The study on prediction method of gas emission amount AQPSO-RBF in fully mechanized mining face and its application [Master's thesis]. Xi'an University of Science and Technology.

[12] Zou, Q., Chen, Z., Cheng, Z., Liang, Y., Xu, W., Wen, P., Zhang, B., Liu, H., & Kong, F. (2022). Evaluation and intelligent deployment of coal and coalbed methane coupling coordinated exploitation based on Bayesian network and cuckoo search. International Journal of Mining Science and Technology, 32, 1315–1328.

[13] Zhou, J., Lin, H., Jin, H., Li, S., Yan, Z., & Huang, S. (2022). Cooperative prediction method of gas emission from mining face based on feature selection and machine learning. International Journal of Coal Science & Technology, 9, 51.

[14] Zhao, W., Dong, H., Ren, J., Yuan, Y., Wang, K., & Wang, F. (2024). A software for calculating coal mine gas emission

quantity based on the different-source forecast method. International Journal of Coal Science & Technology, 11, 51.

[15] Zhang, B., Wang, H., Wang, P., Yu, G., & Gu, S. (2023). Experimental and theoretical study on the dynamic effective stress of loaded gassy coal during gas release. International Journal of Mining Science and Technology, 33, 339–349.